CHALMERS
UNIVERSITY OF TECHNOLOGY

Hypergraph-Based Unified Model Development for Active Battery Equalization Systems

Citation for the original published paper (version of record):
Ouyang, Q., Ghaeminezhad, N., Li, Y. et al (2024). Hypergraph-Based Unified Model Development for Active Battery Equalization Systems. American Control Conference.
http://dx.doi.org/10.23919/ACC60939.2024.10644271

(article starts on next page)

2024 American Control Conference (ACC)
July 8-12, 2024. Toronto, Canada

Hypergraph-Based Unified Model Development for Active Battery Equalization Systems

Quan Ouyang[1], Nourallah Ghaeminezhad[2], Yang Li[1], Torsten Wik[1], and Changfu Zou[1]

***Abstract*— Pack-level battery usage and the inherent cell heterogeneity necessitate effective active equalization systems to enhance their usable capacity and lifetime. Due to the lack of a unified mathematical model, it is difficult to quantitatively analyze and compare the performance of state-of-the-art active equalization systems at the pack level. To address this gap, we introduce a novel, hypergraph-based approach to establish the first unified model for various active battery equalization systems. This model reveals the intrinsic relationship between battery cells and equalizers by representing them as the vertices and hyperedges of hypergraphs, respectively. It can offer a convenient and concise format for comprehensive analysis and comparison. Extensive results demonstrate the efficiency of the proposed model.**

I. Introduction

The demand for high-performance lithium-ion battery systems has grown exponentially with their widespread adoption in electric vehicles and energy storage systems. Since a single lithium-ion battery cell's voltage is limited to 2.4–4.2V due to its inherent electrochemical characteristics, a large number of cells are usually connected in series and parallel in a battery pack to meet the high-voltage and large-capacity requirement for practical applications [1]. However, cell imbalances caused by inhomogeneous conditions and manufacture variations result in insufficient energy use, accelerated capacity degradation, and even safety hazards of the entire battery pack [2]. Thus, the battery pack necessitates an active battery equalization system that can transfer energy from cells with high state-of-charge (SOC) to cells with low SOC.

Numerous active battery equalization systems have been developed to converge the SOC levels of cells within battery packs [3]. Extensive research has focused on the hardware aspects of these systems, exploring various circuit designs, including multi-winding transformers [4] and isolated modified buck-boost converters [5]. Additionally, effective control strategies have been proposed, such as the quasi-sliding mode control [6] and two-layer model predictive control algorithms [7].

Compared to these achievements, much less attention has been focused on quantitative analysis of different equalization systems at the pack level, which, however, is crucial in performance evaluation and comparison of different equalization structures. As one of the few examples, Chen *et al.* quantitatively compared the system-level performance of three types of active equalization structures, using three individually developed models [8]. As an extension, the mathematical models of seven balancing structures were comprehensively reviewed in [9]. A similar work was carried out in [10], where nine analytical algorithms were proposed to estimate the equalization time of different active balancing structures. However, all the referred models are based on analyzing the total equalization currents received by each battery cell under specific structures of the equalization system, which will inevitably fail to capture the system characteristics at the battery pack level, rendering them incapable of mutual expansion and generalization.

To bridge this identified research gap, this paper introduces a unified modeling framework for active battery equalization systems grounded in hypergraph theory. The resulting model reveals the intrinsic relationship between cells and equalizers, in which the equalizers and cells are represented as hyperedges and vertices, respectively. This model can offer a clear and concise way to systematically and comprehensively compare the performance of different active battery equalization systems.

The remainder of this paper is organized as follows. Section II provides an overview of active battery equalization systems. In Section III, the unified active battery equalization model based on hypergraphs is developed. Section IV presents the equalization time estimation and comparison based on the developed unified model. Detailed simulation results and discussions can be found in Section V, followed by conclusions in Section VI.

II. Active Equalization Systems and Their Analysis

The active battery equalization systems adopt several equalizers to transfer extra energy from the cells with high SOC to the ones with low SOC.

A. Overview of State-of-The-Art Active Equalization Systems

Six typical active equalization systems are briefly introduced here as illustrated in Fig. 1, while more comprehensive reviews of battery equalization systems can be found in [9] and [10].

1) Series-based cell-cell (CC) equalization system. Each CC equalizer connects a pair of adjacent cells and transfers energy between them. For a battery pack

This work was supported by Marie Sklodowska-Curie Actions Postdoctoral Fellowships under the Horizon Europe programme (Grant No. 101067291). (Corresponding author: Changfu Zou)

[1]Quan Ouyang, Yang Li, Torsten Wik, and Changfu Zou are with the Department of Electrical Engineering, Chalmers University of Technology, 41296 Gothenburg, Sweden. (e-mail: quano@chalmers.se; yangli@ieee.org; tw@chalmers.se; Changfu.zou@chalmers.se)

[2]Nourallah Ghaeminezhad is with the College of Automation Engineering, Nanjing University of Aeronautics and Astronautics, Nanjing 211100, China. (e-mail: ghaemi@nuaa.edu.cn)

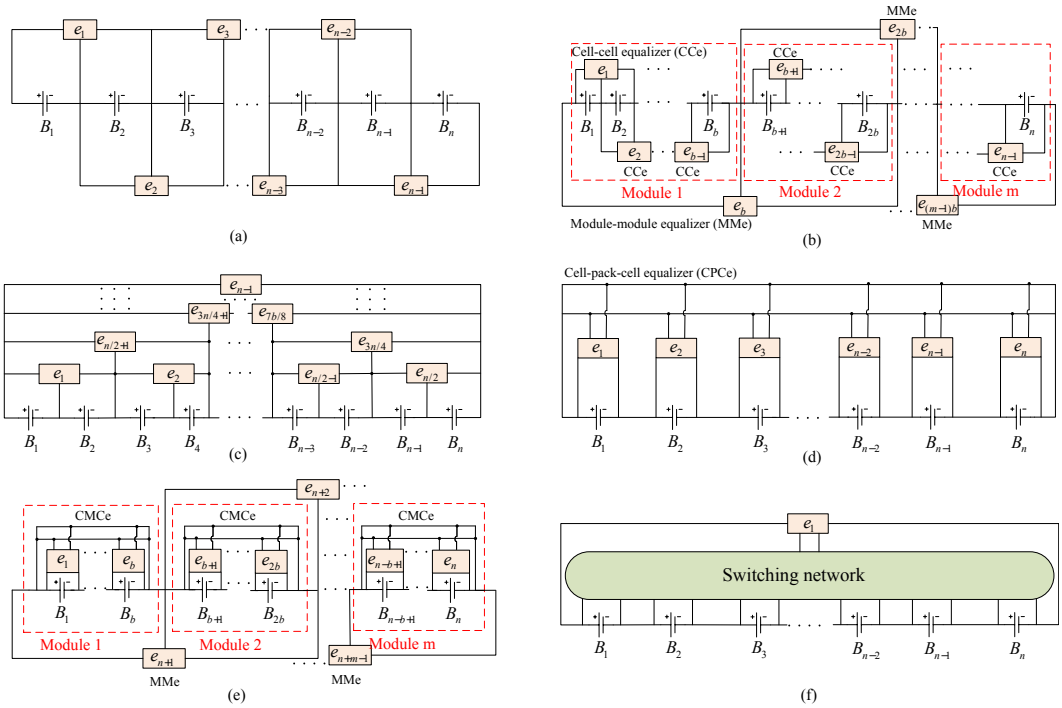

Fig. 1. (a) Series-based CC, (b) module-based CC, (c) layer-based CC, (d) CPC, (e) module-based CPC, and (f) switch-based CPC equalization systems.

with n series-connected cells, $n-1$ CC equalizers are required.

2) Module-based CC equalization system. The battery pack is divided into m series-connected modules, where each battery module contains $b = \frac{n}{m}$ series-connected cells. It enables balancing operations similar to the series-based CC equalization system within each module, while also taking into account neighboring modules for balancing.
3) Layer-based CC equalization system. This system employs a binary-tree-based structure, with multiple layers containing different numbers of equalizers according to the layer number. In each layer, two adjacent cells or modules are connected to the CC or MM equalizers to achieve balancing.
4) Cell-pack-cell (CPC) equalization system. There exist n CPC equalizers for the battery pack with n series-connected cells, where each CPC equalizer connects each cell and the entire battery pack. Energy is transferred between the cell and the battery pack by the CPC equalizer when the cell's SOC is different from the average SOC of the battery pack.
5) Module-based CPC equalization system. The battery pack is divided into m modules, similar to the module-based CC equalization system. In each module, cell-module-cell (CMC) equalizers are utilized to perform the same operation as in the CPC equalization system to achieve equalization.
6) Switch-based CPC equalization system. All battery cells share one CPC equalizer, and a switching network controls which cell is connected to the equalizer. This structure allows bidirectional energy transfer between any selected cell and the battery pack.

As far as we know, in the existing work comparing different equalization systems, such as [9]–[11], the different battery equalization systems are modeled separately, and then individually tailored models are utilized to simulate and evaluate the performance of each system. This is mainly because most models of active battery equalization were developed by analyzing the total equalization currents received by each battery cell under a specific equalization structure. cumbersome and complex.

B. Equalization Current Analysis

According to Section II-A, the equalizers include CC, MM, CPC, and CMC equalizers, depending on the number of cells they are connected to. The six equalization systems mentioned above are combinations of these four types of equalizers.

1) Equalization currents through CC equalizers: To achieve battery equalization, a CC equalizer transfers energy from its connected cell with a high SOC to the other cell with a low SOC. In this study, we define the discharging current as positive and the charging current as negative. Also, the cells' SOC information is assumed to be available. Referring to [8], for the l-th CC equalizer connected with the i-th and j-th battery cells, it can be obtained that

$$I_{ec_{i,l}}(k) = I_{ec_l}(k) \tag{1a}$$
$$I_{ec_{j,l}}(k) = -I_{ec_l}(k) \tag{1b}$$

where $I_{ec_{i,l}}$ denotes the i-th cell's equalization current through the l-th CC equalizer, I_{ec_l} is the directed equalization current provided by the l-th CC equalizer, which is commonly defined as [8]–[11]

$$I_{ec_l}(k) = \text{sgn}(SOC_i(k) - SOC_j(k))\bar{I}_{ec_l}(k) \tag{2}$$

where $\text{sgn}(\cdot)$ is the sign function and $\bar{I}_{ec_l}(k) \geq 0$ is the magnitude of the equalization current. Note that for a CC equalizer in the series-based and module-based CC equalization systems, as shown in Fig. 1(a–b).

2) Equalization currents through MM equalizers: Similar to CC equalizers, an MM equalizer transfers energy from its connected module with a high average SOC to the other module with a low average SOC. Consider the l-th MM equalizer connected to the i-th battery module containing b series-connected cells labeled $\{c, c+1, \cdots, c+b-1\}$ and the j-th battery module containing another b series-connected cells $\{d, d+1, \cdots, d+b-1\}$, where c and d are the cell starting indices in the corresponding modules. Because of the series connections, the same current goes through all cells in the module, the cell equalization currents through this MM equalizer can be expressed as

$$\begin{aligned} I_{em_{c,l}}(k) &= I_{em_{c+1,l}}(k) = \cdots = I_{em_{c+b-1,l}}(k) \\ &= I_{em_l}(k) \end{aligned} \tag{3a}$$

$$\begin{aligned} I_{em_{d,l}}(k) &= I_{em_{d+1,l}}(k) = \cdots = I_{em_{d+b-1,l}}(k) \\ &= -I_{em_l}(k). \end{aligned} \tag{3b}$$

Similar to CC equalizers, I_{em_l} is usually designed as

$$I_{em_l}(k) = \text{sgn}(S\bar{O}C_{m_i}(k) - S\bar{O}C_{m_j}(k))\bar{I}_{em_l}(k) \tag{4}$$

where $\bar{I}_{em_l}(k) \geq 0$. The average SOCs of the i-th and j-th battery modules $S\bar{O}C_{m_i}$ and $S\bar{O}C_{m_j}$ are defined by $S\bar{O}C_{m_i}(k) = \frac{1}{b}\sum_{q=c}^{c+b-1} SOC_q(k)$ and $S\bar{O}C_{m_j}(k) = \frac{1}{b}\sum_{q=d}^{d+b-1} SOC_q(k)$. Note that the MM equalizers are utilized in the module-based CC, layer-based CC, and module-based CPC equalization systems, as shown in Fig. 1(b-c, e).

3) Equalization currents through CPC equalizers: The CPC equalizer l enables energy transfer between its connected cell i and the battery pack whenever their SOC difference exceeds a given small threshold. The equalization current on the pack side is $\frac{1}{n}$ of the equalization current on the cell side. Moreover, since the i-th cell is included in the battery pack, it also receives the same equalization current on the side of the battery pack. Hence, the cell's equalization current through the l-th CPC equalizer $I_{ep_{p,l}}$ $(1 \leq p \leq n)$ can be calculated by [9]

$$I_{ep_{p,l}}(k) = \begin{cases} \frac{n-1}{n} I_{ep_l}(k), & p = i \\ -\frac{1}{n} I_{ep_l}(k), & p = 1, 2, \cdots, n, p \neq i \end{cases} \tag{5}$$

where I_{ep_l} is commonly designed as

$$I_{ep_l}(k) = \text{sgn}(SOC_i(k) - S\bar{O}C_P(k))\bar{I}_{ep_l}(k) \tag{6}$$

with $\bar{I}_{ep_l}(k) \geq 0$. The average SOC of the battery pack $S\bar{O}C_P$ is defined as $S\bar{O}C_P(k) = \frac{1}{n}\sum_{i=1}^{n} SOC_i(k)$. Note that a CPC equalizer will generate unequal equalization currents on its connected cell and battery pack. CPC equalizers can be seen in the CPC, module-based CPC, and switch-based CPC equalization systems, as illustrated in Fig. 1(d–f).

4) Equalization currents through CMC equalizers: The CMC equalizers have the same structure as the CPC equalizers. Their only difference is that one side of the CMC equalizer is connected to the battery module instead of the entire battery pack. For the l-th CMC equalizer connected to the i-th cell and the j-th battery module (containing cells $c, \cdots, i, \cdots, c+b-1$), similar to (5), the cell equalization current through the l-th CMC equalizer $I_{ecm_{p,l}}$ $(c \leq p \leq c+b-1)$ is

$$I_{ecm_{p,l}}(k) = \begin{cases} \frac{b-1}{b} I_{ecm_l}(k), & p = i \\ -\frac{1}{b} I_{ecm_l}(k), & p = c, \cdots, c+b-1, p \neq i \end{cases} \tag{7}$$

where I_{ecm_l} is usually designed as

$$I_{ecm_l}(k) = \text{sgn}(SOC_i(k) - S\bar{O}C_{m_j}(k))\bar{I}_{ecm_l}(k) \tag{8}$$

with $\bar{I}_{ecm_l}(k) \geq 0$. The CMC equalizers are utilized in the module-based CPC equalization system, as shown in Fig. 1(e).

III. Unified Model Development For Active Battery Equalization Systems

A. Hypergraph representation of equalizers and cells

To uncover the intrinsic connection between battery cells and equalizers, the cells are regarded as the vertices, and the equalizers that transfer energy between cells are treated as edges. Note that the MM, CPC, and CMC equalizers are connected to more than two battery cells, as seen in Fig. 1, which means that an edge connects several vertices. These edges are called hyperedges in the concept of hypergraphs [12]. For an active equalization system with n_e equalizers for a battery pack with n series-connected cells, the battery cells are labelled as $B_1, \cdots, B_n$, the CC equalizers are labelled as $e_1, \cdots, e_{n_1}$, the MM equalizers are labelled as $e_{n_1+1}, \cdots, e_{n_2}$, the CPC equalizers are labelled as $e_{n_2+1}, \cdots, e_{n_3}$, and the CMC equalizers are labelled as $e_{n_3+1}, \cdots, e_{n_e}$, respectively. Then, the active equalization system can be represented by a hypergraph $G = (\nu, \varepsilon)$ with the vertex set $\nu = \{B_1, B_2, \cdots, B_n\}$ and the hyperedge set $\varepsilon = \{e_1, e_2, \cdots, e_{n_e}\}$.

The hyperedges e_l $(1 \leq l \leq n_e)$ are ordered pairs of disjoint subsets of vertices, denoted as $e_l = \{H(e_l), T(e_l)\}$, where $H(e_l)$ and $T(e_l)$ denote the head and tail of e_l, respectively [13]. The element of the incidence matrix $C \in \mathbb{R}^{n \times n_e}$ of the hypergraph G, denoted as $c_{p,l}$ $(1 \leq p \leq n, 1 \leq l \leq n_e)$, can then be defined as

$$c_{p,l} = \begin{cases} w_{l_h}, & \text{if } B_p \in H(e_l) \\ w_{l_t}, & \text{if } B_p \in T(e_l) \\ 0, & \text{otherwise} \end{cases} \tag{9}$$

where w_{l_h} and w_{l_t} are the weights. To visualize the hypergraphs, in Fig. 2, each hyperedge is represented as a big

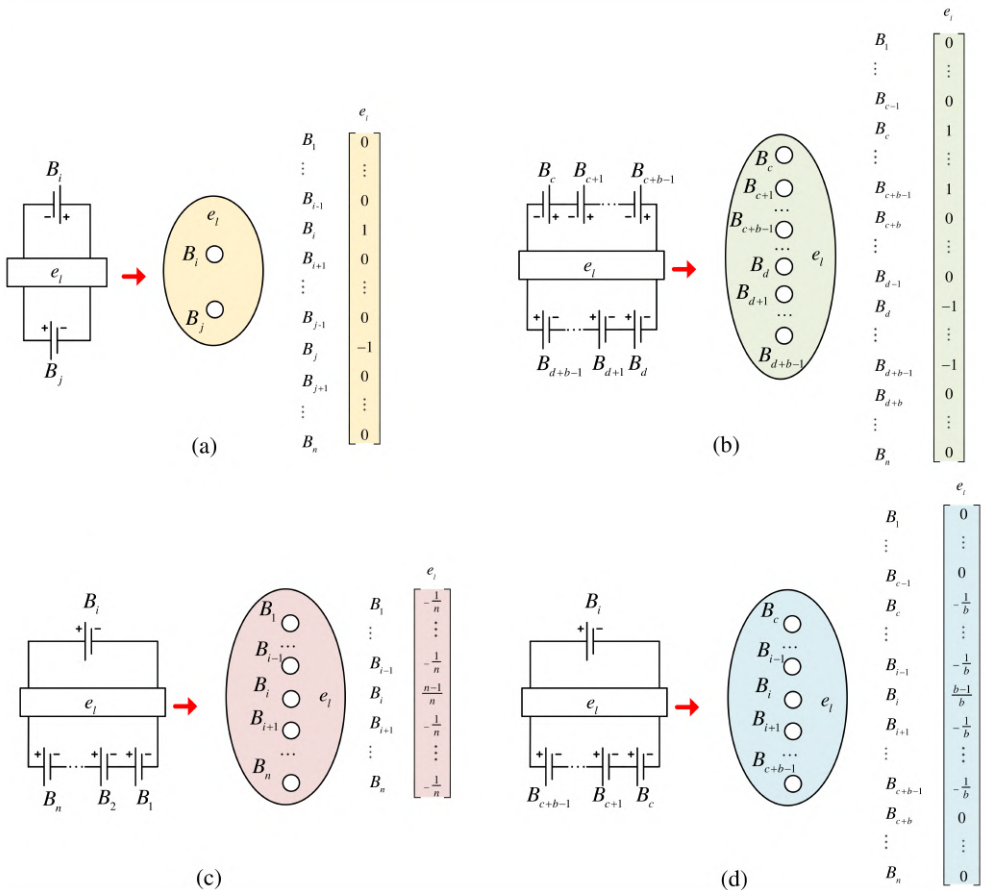

Fig. 2. Electric circuit presentation and equivalent hyperedge of different equalizers: (a) CC, (b) MM, (c) CPC, and (d) CMC equalizers.

ellipse distinguished by different colors, enclosing all the connected vertices. Without loss of generality, we define the top subsets of cells in Fig. 2 as the heads and the bottom subsets as the tails. The incidence vector corresponding to the hyperedge e_l, denoted as $c_l \in \mathbb{R}^n$, can be generally formulated as

$$\begin{aligned} c_l &= [c_{1,l}, c_{2,l}, \cdots, c_{n,l}]^T \\ &= [\cdots, 0, \underbrace{w_{l_h}, \cdots, w_{l_h}}_{B_i \in H(e_l)}, 0, \cdots, 0, \underbrace{w_{l_t}, \cdots, w_{l_t}}_{B_j \in T(e_l)}, 0, \cdots]^T. \end{aligned} \tag{10}$$

The weights w_{l_h} and w_{l_t} can be derived based on the relationship between the equalizing currents on both sides of the equalizer.

B. Application of hypergraphs to equalizer modeling

By using the hypergraph theory and its properties described in Section III-A, a unified model can be developed for all the active battery equalization systems. According to the definition of the incidence matrix in the hypergraph theory, the equalization current received by cell p from equalizer l satisfies

$$I_{e_{p,l}}(k) = c_{p,l} I_l(k) \tag{11}$$

where I_l represents the directed equalization current provided by equalizer l in any type of active equalization system. For example, I_l can be embodied as I_{ec_l}, I_{em_l}, I_{ep_l}, and I_{ecm_l}. By vectorizing the equalization current received by the in-pack battery cell from equalizer l as $I_{e_l} = [I_{ec_{1,l}}, \cdots, I_{ec_{n,l}}]^T$, based on (11), it yields

$$I_{e_l}(k) = c_l I_l(k). \tag{12}$$

1) Hypergraph-based modeling of CC equalizers: For the CC equalizer (hyperedge) e_l $(1 \le l \le n_1)$, as shown in Fig. 2(a), we have $H(e_l) = \{B_i\}$, and $T(e_l) = \{B_j\}$. As per (10), we can obtain

$$c_l = [\cdots, 0, \underbrace{w_{l_h}}_{p=i}, 0, \cdots, 0, \underbrace{w_{l_t}}_{p=j}, 0, \cdots]^T. \tag{13}$$

Based on (1) and (11), it can be concluded that $w_{l_h} = 1, w_{l_t} = -1$. In fact, for any CC equalizer e_l connecting cell i and j,

$$I_{e_l}(k) = [\cdots, 0, \underbrace{1}_{p=i}, 0, \cdots, 0, \underbrace{-1}_{p=j}, 0, \cdots]^T I_{ec_l}(k) \tag{14}$$

where $1 \le l \le n_1$.

2) Hypergraph-based models of other equalizers: For the MM equalizer e_l $(n_1+1 \le l \le n_2)$ illustrated in Fig. 2(b), $H(e_l)=\{B_c, B_{c+1}, \cdots, B_{c+b-1}\}$ and $T(e_l)=\{B_d, B_{d+1}, \cdots, B_{d+b-1}\}$. For the CPC equalizer e_l $(n_2+1 \le l \le n_3)$ Fig. 2(c), $H(e_l)=\{B_i\}$, $T(e_l)=\{B_1, \cdots, B_{i-1}, B_{i+1}, \cdots, B_n\}$. For the CMC equalizer e_l $(n_3+1 \le l \le n_e)$ illustrated in Fig. 2(d), $H(e_l)=\{B_i\}$, $T(e_l)=\{B_c, \cdots, B_{i-1}, B_{i+1}, \cdots, B_{c+b-1}\}$. By using the same procedure as in Section III-B.1, we can obtain

$$I_{e_l}(k)=[\ \cdots,0,\ \underbrace{1,\ldots,1}_{p=c,\cdots,c+b-1},\ 0\ldots,0,\ \underbrace{-1,\ldots,-1}_{p=d,\cdots,d+b-1},\ 0,\cdots]^T I_{em_l}(k),\ \ n_1+1\le l\le n_2 \tag{15}$$

$$I_{e_l}(k)=[\underbrace{-\frac{1}{n},\cdots,-\frac{1}{n}}_{p=1,\cdots,i-1},\underbrace{\frac{n-1}{n}}_{p=i},\underbrace{-\frac{1}{n},\ldots,-\frac{1}{n}}_{p=i+1,\cdots,n}]^T \times I_{ep_l}(k),\ \ n_2+1\le l\le n_3 \tag{16}$$

$$I_{e_l}(k)=[\ \cdots,0,\underbrace{-\frac{1}{b},\cdots,-\frac{1}{b}}_{p=c,\cdots,i-1},\underbrace{\frac{b-1}{b}}_{p=i},\ \underbrace{-\frac{1}{b},\ldots,-\frac{1}{b}}_{p=i+1,\cdots,c+b-1},\ 0,\cdots]^T I_{ecm_l}(k),\ \ n_3+1\le l\le n_e \tag{17}$$

C. Hypergraph-based battery system modeling

According to Coulomb counting, the dynamics of the i-th $(1 \le i \le n)$ cell's SOC in the battery pack can be described by [14]:

$$SOC_i(k+1)=SOC_i(k)-\frac{\eta T_0}{3600Q_i}(I_s(k)+I_{eq_i}(k)) \tag{18}$$

where Q_i and I_{eq_i} are the ampere-hour capacity and total equalizing current of cell i, T_0 denotes the sampling period, η represents the coulombic efficiency, and I_s is the current of the battery pack through the external power source or load, which is the same for all cells due to their series connection. Based on the equalization currents in (14)–(17), the total equalization current vector for the cells in the battery pack $I_{eq}=[I_{eq_1}, I_{eq_2}, \cdots, I_{eq_n}]^T$ can be calculated as

$$I_{eq}(k)=\sum_{l=1}^{n_1} c_l I_{ec_l}(k)+\sum_{l=n_1+1}^{n_2} c_l I_{em_l}(k) + \sum_{l=n_2+1}^{n_3} c_l I_{ep_l}(k)+\sum_{l=n_3+1}^{n_e} c_l I_{ecm_l}(k). \tag{19}$$

Then, by defining the state vector $x(k)$, the diagonal matrix D, the vector $d(k)$, and the control variable vector $u(k)$ as $x(k)=[SOC_1(k), SOC_2(k), \cdots, SOC_n(k)]^T \in \mathbb{R}^n$, $D=\text{diag}\left\{\frac{\eta T_0}{3600Q_1}, \cdots, \frac{\eta T_0}{3600Q_n}\right\} \in \mathbb{R}^{n\times n}$, $d(k)=[I_s(k), \cdots, I_s(k)]^T \in \mathbb{R}^n$, $u(k)=[I_{ec_1}(k), \cdots, I_{ec_{n_1}}(k), I_{em_{n_1+1}}(k), \cdots, I_{em_{n_2}}(k), I_{ep_{n_2+1}}(k), \cdots, I_{ep_{n_3}}(k), I_{ecm_{n_3+1}}(k), \cdots, I_{ecm_{n_e}}(k)] \in \mathbb{R}^{n_e}$, where $\text{diag}(\cdot)$ represents a diagonal matrix, the unified model for battery equalization systems can be formulated in the following state-space form:

$$x(k+1)=x(k)-DCu(k)-Dd(k) \tag{20}$$

where $C=[c_1, \cdots, c_{n_e}]$ is the incidence matrix.

IV. Equalization Time Estimation Based on Unified Model

Based on the formulated unified model (20), the equalization time of each battery equalization system can be estimated and compared conveniently. The equalization time can be defined as:

$$T_e=\min\{\tau : \tfrac{1}{n}||x(k)-\bar{x}(k)|| \le \epsilon, \forall k T_0 \ge \tau\} \tag{21}$$

where $||\cdot||$ stands for the 2-norm, $\bar{x}(k)=\frac{1}{n}1_n 1_n^T x(k)$, and ϵ is the upper bound of SOC imbalance tolerance. Below, Algorithm 1 is proposed to estimate the equalization time.

Algorithm 1

1) Set the cells' capacity Q_i and initial state-of-charge, $SOC_i(0)$ $(1 \le i \le n)$, the tolerance bound ϵ, and the sampling period T_0.
2) Based on the connection of CC/MM/CPC/CMC equalizers, set the vectors c_l $(1 \le l \le n_e)$ through (10) to obtain the incidence matrix $C=[c_1, \cdots, c_{n_e}]$.
3) Iterate $x(k)$ based on the state-space model (20) while ignoring the external current, i.e., setting $d(k)=0_n$.
4) Terminate and output $T_e=kT_0$, if $\frac{1}{n}||x(k)-\bar{x}(k)|| \le \epsilon$. Otherwise, set $k=k+1$ and return to Step 2).

As seen in the literature works [8], [10], each equalization system needs a specific estimation algorithm for its equalization time, making it inconvenient for the systematic comparison and advancement of various equalization systems. The issue can be well remedied using Algorithm 1 which uses the unified model for all equalization systems.

V. Model Efficacy Validation Results

MATLAB-based simulations are conducted to evaluate the effectiveness of the proposed unified battery equalization model. The experimental results are taken from [15], in which four battery cells with a capacity of 65Ah were used to generate the SOC evolution trajectories. With the initial SOCs as $x(0)=[62\%, 48\%, 63\%, 42\%]^T$, comparative results between the model-based outputs and measured outputs are presented in Fig. 3, where the experimental SOC was calculated from Coulomb counting, and the fluctuations were due to noise of the utilized current sensors. In addition to series-based CC equalization systems, the proposed model is further assessed on the layer-based CC equalization system, with the results illustrated in Fig. 4. A high level of consistency is achieved between the model's predictions and the experimental data, thereby corroborating the validity of the developed model.

To further test the proposed battery equalization model on other system structures, a battery pack consisting of 12 cells with the capacity of 3.1Ah in [9] is utilized for simulation, where the cells' initial SOC vector is $x(0)=[65\%, 62\%, 85\%, 79\%, 75\%, 63\%, 77\%, 71\%, 82\%, 88\%, 76\%, 68\%]^T$. The simulation results obtained by Algorithm 1 for the module-based CC,

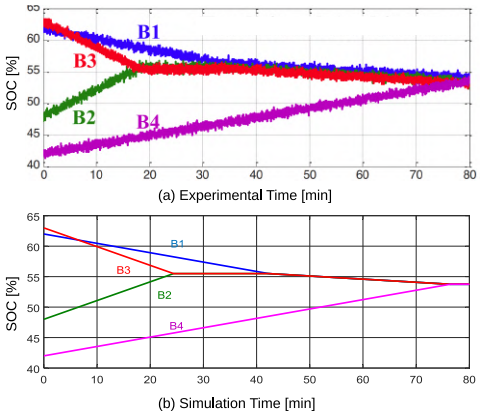

Fig. 3. (a) Experimental result [15], (b) simulation result based on model (20) for a series-based CC equalization system.

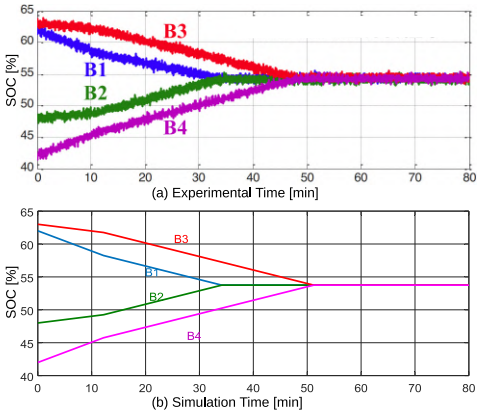

Fig. 4. (a) Experimental result [15], (b) simulation result based on model (20) for a layer-based CC equalization system.

CPC, and module-based CPC systems are illustrated in Fig. 5(a)-(c), which are consistent with those in [9]. The simulation result for the switch-based CPC equalization system is also given in Fig. 5(d).

VI. Conclusion

This study presents a novel hypergraph-based modeling framework for active battery equalization systems, which reveals the inherent relationship between cells and equalizers, facilitating straightforward analysis and comparison of different systems. The obtained unified model can serve as an efficient tool for various model-based applications, e.g., advancing control strategies and driving progress in battery equalization technologies for a sustainable energy transition.

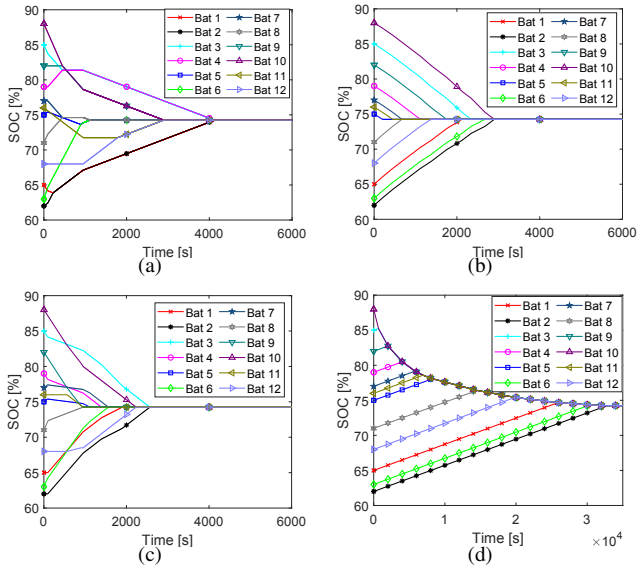

Fig. 5. Simulation results for (a) module-based CC, (b) CPC, (c) module-based CPC, (d) switch-based CPC equalization systems based on model (20).

References

[1] F. Feng, X. Hu, J. Liu, X. Lin, and B. Liu, "A review of equalization strategies for series battery packs: variables, objectives, and algorithms," *Renewable and Sustainable Energy Reviews*, vol. 116, p. 109464, 2019.

[2] C. Jian, O. Quan, and Z. Wang, *Equalization Control for Lithium-ion Batteries*. Singapore: Springer, 2023.

[3] J. Gallardo-Lozano, E. Romero-Cadaval, M. I. Milanes-Montero, and M. A. Guerrero-Martinez, "Battery equalization active methods," *Journal of Power Sources*, vol. 246, pp. 934 – 949, 2014.

[4] Y. Chen, X. Liu, Y. Cui, J. Zou, and S. Yang, "A multiwinding transformer cell-to-cell active equalization method for lithium-ion batteries with reduced number of driving circuits," *IEEE Transactions on Power Electronics*, vol. 31, no. 7, pp. 4916–4929, 2016.

[5] Q. Ouyang, J. Chen, J. Zheng, and H. Fang, "Optimal cell-to-cell balancing topology design for serially connected lithium-ion battery packs," *IEEE Transactions on Sustainable Energy*, vol. 9, no. 1, pp. 350–360, 2018.

[6] Q. Ouyang, J. Chen, J. Zheng, and Y. Hong, "SOC estimation-based quasi-sliding mode control for cell balancing in lithium-ion battery packs," *IEEE Transactions on Industrial Electronics*, vol. 65, no. 4, pp. 3427–3436, April 2018.

[7] Q. Ouyang, Y. Zhang, N. Ghaeminezhad, J. Chen, Z. Wang, X. Hu, and J. Li, "Module-based active equalization for battery packs: A two-layer model predictive control strategy," *IEEE Transactions on Transportation Electrification*, vol. 8, no. 1, pp. 149–159, 2022.

[8] H. Chen, L. Zhang, and Y. Han, "System-theoretic analysis of a class of battery equalization systems: Mathematical modeling and performance evaluation," *IEEE Transactions on Vehicular Technology*, vol. 64, no. 4, pp. 1445–1457, 2015.

[9] N. Ghaeminezhad, Q. Ouyang, X. Hu, G. Xu, and Z. Wang, "Active cell equalization topologies analysis for battery packs: A systematic review," *IEEE Transactions on Power Electronics*, vol. 36, no. 8, pp. 9119–9135, 2021.

[10] F. Qu, Q. Luo, H. Liang, D. Mou, P. Sun, and X. Du, "Systematic overview of active battery equalization structures: Mathematical modeling and performance evaluation," *IEEE Transactions on Energy Conversion*, vol. 37, no. 3, pp. 1685–1703, 2022.

[11] W. Han, C. Zou, C. Zhou, and L. Zhang, "Estimation of cell SOC evolution and system performance in module-based battery charge equalization systems," *IEEE Transactions on Smart Grid*, vol. 10, no. 5, pp. 4717–4728, 2019.

[12] A. Bretto, *Hypergraph Theory: An Introduction*. Cham: Springer, 2013.

[13] G. Gallo, G. Longo, S. Pallottino, and S. Nguyen, "Directed hypergraphs and applications," *Discrete Applied Mathematics*, vol. 42, no. 2, pp. 177–201, 1993.

[14] Q. Ouyang, W. Han, C. Zou, G. Xu, and Z. Wang, "Cell balancing control for lithium-ion battery packs: A hierarchical optimal approach," *IEEE Transactions on Industrial Informatics*, vol. 16, no. 8, pp. 5065–5075, 2020.

[15] B. Dong and Y. Han, "A new architecture for battery charge equalization," in *2011 IEEE Energy Conversion Congress and Exposition*, 2011, pp. 928–934.